ISSN No:-2456-2165

Modelling the Transmission and Control Dynamics of Coronavirus Disease with Social Distancing and Contact Tracing

Moses Olayemi Adeyemi[1], Temitayo Olabisi Oluyo[2] and Janet Kikelomo Oladejo[3]

Department of Pure and Applied Mathematics, Ladoke Akintola University of Technology, PMB 4000, Ogbomoso, NIGERIA

Abstract:- The Coronavirus disease (COVID 19) pandemic is not only a health problem but also a global economic problem, which disrupts the daily life of people around the globe, including billions of children whose education are derailed. We formulate a mathematical model which studies the dynamic of the disease in the presence of preventive measures like social distancing, contact tracing, quarantine and isolation of cases. The model was shown to be biologically feasible and mathematically well-posed, and has both disease-free and endemic equilibria. The basic reproduction number (R_0) was also computed, and a sensitivity analysis was carried out on R_0. Furthermore, numerical simulations were performed to validate the result of the qualitative stability analyses of the equilibria, and to determine the effects of some epidemiological parameters.

It was established that whenever $R_0 < 1$, the disease-free equilibrium is both locally and globally asymptotically stable and no endemic equilibrium, while when $R_0 > 1$, the disease-free equilibrium is unstable and the endemic equilibrium is asymptotically stable both locally (with conditions) and globally. The sensitivity analysis showed that rate of social distancing and effective contact rate are the most sensitive parameters to R_0, among others. The results of the numerical simulations showed that increase in the rate of effective contact causes increase in COVID-19 epidemic, while increase in the rates of social distancing, contact tracing, quarantine, isolation of cases and recovery decline the epidemic.

Therefore, a high social distancing should be maintained as intensive contact tracing followed by quarantine, isolation of cases and supportive treatment are in place as intervention measures, in order to keep the epidemic under control.

Keywords—*Corona Virus, COVID-19, Social distancing, Contact tracing, Quarantine, Isolation, Reproduction number, Equilibrium, Stability, Sensitivity*

I. INTRODUCTION

The new strain of Corona virus, Severe Acute respiratory syndrome Corona virus 2 (SARS-CoV-2) first identified in Wuhan china, in December 2019, is the causative agent of Corona virus disease 2019 (COVID-19), and is highly infectious [1]. The origin of the zoonotic virus is yet to be confirmed, studies revealed that SARS-CoV-2 likely originated in bat, SARS-CoV-2 isolated from infected human is closely related genetically to corona virus from bats population [2,3]. Evidences from reported cases show that incubation period of COVID-19 ranges from 1-14 days. It was also discovered that the duration between exposures to the onset of infectiousness (latent period) may be shorter than incubation period. In essence asymptomatic and symptomatic persons can transmit the disease [4,5]. Based on current research report, SARS-CoV-2 is transmitted through particle droplets called aerosols, fomites, and close contact with an infected person or surfaces [6], also with possible spread through faeces [7]. The virus as reported can remain on surfaces for up to 9 days, aerosols and droplets produced through sneezing or speech can be inhaled by susceptible persons. Upon inhalation the particles are deposited in the upper region of the respiratory lungs, from which may be expelled or swallowed [8]. This informed the advisability of wearing a suitable mask and allowing for adequate ventilation of enclosed places.

There is no cure or specific antiretroviral treatment recommended for COVID-19 and no vaccine is presently available but understudy. Instead, infected persons receive treatments that manage symptoms as the virus runs its course. Therefore, avoidance is the principal cure. The symptoms of covid-19 could be mild or moderate respiratory illness, individuals recover with or without special treatment except those with medical conditions such as lungs, kidney or heart diseases, immune system condition such as HIV/AIDS and diabetes. The symptoms include fever, tiredness, coughing, and shortness of breath, sore throat and acute respiratory syndrome in severe cases [9].

Since the emergence, in late 2019, of the novel SARS-CoV-2 that causes COVID-19 there have been 2.6million confirmed cases including more than 180 thousand deaths recorded worldwide [10]. The Corona virus disease (COVID 19) pandemic is not only a health problem but also an economic problem, daily life of people around the globe are disrupted including billions of children whose education are derailed and the breakout of domestic violence amid the lockdown. Prevention and control of the new disease can be done if new infections are controlled, with adequate contact tracing, isolation and quarantine also maintaining good

personal and environmental hygiene [11]. Despite the increase in the number of infected persons worldwide especially in the Sub Sahara Africa the World Health Organization (WHO) in a press briefing in April 2020 to Africa says containment is possible and will require adequate testing, hand washing, making treatment centres available to care for infected patient appropriately, maintaining social distancing and obey the stay-at-home order [12]. Likewise a recent research by the Imperial College London research team reported that Africa could see about 3.3million death and 1.2 billion infections within 3 to 6 months if the virus is left unchecked. The team suggested that rapid adoption of proven health measures including testing, isolation of cases and wider social distancing to prevent onward transmission are critical in curbing the impact of the pandemic [13].

A number of mathematical models have been developed to better understand the dynamics and investigate how to effectively control the spread of COVID 19. Kucharski *et al.* [14] modelled the early dynamics of transmission and control of the disease, they combined a SEIR model of SARS-CoV-2 transmission with four datasets from within and outside Wuhan to estimate how the transmission in Wuhan changed from December 2019 to January 2020. The estimates were used to assess the potential for sustained human to human transmission to occur in locations outside Wuhan if cases were introduced. Their results also show that there was probably substantial variation in SARS-CoV-2 transmission over time; sudden decline in transmission in Wuhan coincides with travel control measures. Tang *et al.* [15] devised an SEIR compartmental model based on the clinical progression of COVID-19, epidemiological status of the individual and intervention. They reported that the intervention can effectively reduce the control reproduction number and transmission risk. In an updated version of the previous model, Tang *et al*. [16] stated that policy decision of the major public health intervention such as contact tracing, quarantine and isolation are not enough to reduce the trend of the peak time of the epidemic but require real time information of the data, knowledge about the implementation and the resources available to facilitate the implementation of such intervention. Okhuese [17] in an effort to evaluate the disease equilibrium proposed a model for COVID -19 agreeing that unless there is a dedicated effort from government, decision makers and the stakeholders eminent spread cannot be avoided. Other researches on mathematical modelling of COVID-19 can be seen [18–24].

In the present work, we formulate a mathematical model, using a system of ordinary differential equations to study the dynamic of COVID-19 in the presence of preventive measures like social distancing, contact tracing, quarantine, isolation of cases and supportive treatment. The rest of this work is organized as follows: we give a full description of the model and show a domain where the model is biologically feasible and mathematically well posed in Section II. Section III provides the existence of equilibria including a derivation of the basic reproduction number and stability analysis of the equilibria. In Section IV, we perform sensitivity analysis and numerical simulations of the model with graphical illustrations and their discussion, and give concluding remark in Section V.

II. MODEL FORMULATION AND PROPERTIES

To study the dynamical transmission and control of Corona virus disease, an epidemic mathematical model was formulated.

A. *Formulation of the Model*

This new model subdivides the total human population size at time *t*, denoted by $N(t)$, into individuals who are susceptible $S(t)$; exposed $E(t)$; quarantined $Q(t)$; infected $I(t)$; isolated $J(t)$; and recovered $R(t)$, so that

$$N(t) = S(t) + E(t) + Q(t) + I(t) + J(t) + R(t) \ . \qquad (1)$$

Susceptible individuals are recruited into the population either by birth or immigration at a rate Π. When a susceptible individual get into effective contact with any of the infectious individuals, the susceptible individual contracts the corona virus and move to the exposed compartment at a rate $(1-\eta)\beta\left(\frac{\varepsilon_1 Q(t) + I(t) + \varepsilon_1 J(t)}{N}\right)S(t)$, where ε_1 and ε_2 are infectivity reduction rates in quarantined and isolated sub-populations respectively due to hygiene precautions, and η is the rate of social distancing, which accounts for a reduction the contact. The susceptible class is further reduced by natural mortality at a rate μ and increased by $(1-\xi)\sigma Q(t)$ and $\kappa R(t)$, $(1-\xi)\sigma$ is a proportion of the quarantined individuals who are uninfected after their quarantine period, and κ is immunity loss rate after recovery which is responsible for re-infection.

Contacts with the exposed and infected individuals are traced at a rate τ_1 and τ_2, and such traced individuals are respectively quarantined or isolated. The exposed is further reduced by $(\mu+\rho)E(t)$, where $1/\rho$ is the average time spent in the latency period. A detected proportion of $\theta\rho$ of the exposed are quarantined after latency period while the other proportion $(1-\theta)\rho$ moves to the infected class. The quarantined and the infected classes are further reduced by $(\mu+\sigma)Q(t)$ and $(\mu+\delta_1+\tau_2+\gamma_1)I(t)$ respectively, where δ_1 and γ_1 are COVID-19 related mortality and progression rates of the infected respectively. The isolated and recovered classes are increased by

$\xi\sigma Q(t)+(\tau_2+\varphi\gamma_1)I(t)$ and $(1-\varphi)\gamma_1 I(t)+\gamma_2 J(t)$ respectively, where $\varphi\gamma_1$ are the proportion of infected who are isolated upon detection and $(1-\varphi)\gamma_1$ are the other proportion who recovered. These two classes are reduced by $(\mu+\delta_2+\gamma_2)J(t)$ and $(\mu+\kappa)R(t)$ respectively, where δ_2 and γ_2 are the COVID-19 related mortality and recovery rates for the isolated classes.

It is assumed that exposed individuals do not always transmit COVID-19, since they do not show symptoms [25], and works are still on-going as to whether they actually transmit or not. Even if they do, it is with reduced infectivity. It should be noted that exposed individuals differ from asymptomatic infective individuals. Also, on the basis of the fact that the on-going pandemic of COVID-19 spread majorly through person-person transmission [23, 26], the population of virus in the environment is not considered in the model.

The Fig. 1 below shows the dynamics of the model with the inflow and outflow of individuals in each compartment with detail of the model parameters given in Table 1.

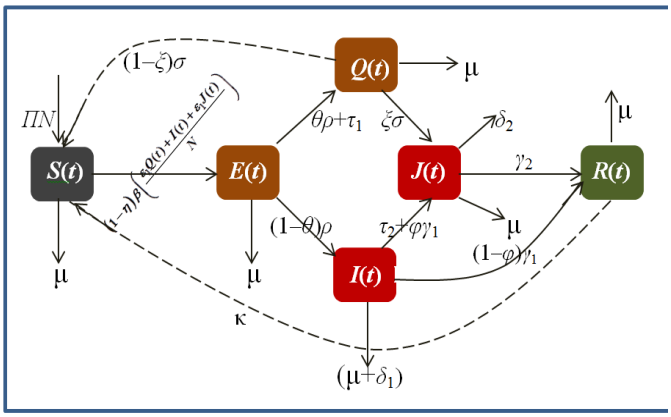

Fig. 1: *Schematic diagram showing the dynamics of COVID-19 in human population*

The model is mathematically formulated as a system of coupled ordinary differential equations as:

$$\begin{aligned}
\frac{dS(t)}{dt} &= \Pi N-\mu S(t)-(1-\eta)\beta\left(\frac{\varepsilon_1 Q(t)+I(t)+\varepsilon_1 J(t)}{N}\right)S(t)+(1-\xi)\sigma Q(t)+\kappa R(t)\\
\frac{dE(t)}{dt} &= (1-\eta)\beta\left(\frac{\varepsilon_1 Q(t)+I(t)+\varepsilon_1 J(t)}{N}\right)S(t)-(\mu+\tau_1+\rho)E(t)\\
\frac{dQ(t)}{dt} &= (\theta\rho+\tau_1)E(t)-(\mu+\sigma)Q(t)\\
\frac{dI(t)}{dt} &= (1-\theta)\rho E(t)-(\mu+\delta_1+\tau_2+\gamma_1)I(t) \qquad (2)\\
\frac{dJ(t)}{dt} &= \xi\sigma Q(t)+(\tau_2+\varphi\gamma_1)I(t)-(\mu+\delta_2+\gamma_2)J(t)\\
\frac{dR(t)}{dt} &= (1-\varphi)\gamma_1 I(t)+\gamma_2 J(t)-(\mu+\kappa)R(t);
\end{aligned}$$

with

$$S(t_0)=S_0, E(t_0)=E_0, Q(t_0)=Q_0, I(t_0)=I_0, J(t_0)=J_0, R(t_0)=R_0. \qquad (3)$$

B. Normalization of the Model Equations

A constant population is assumed (i.e. $N(t) = N$ is a constant). Hence, without loss of generality, a dimensionless system can be used to explore the dynamics of the COVID-19 model.

***Table* 1:** *Description of the Model's Variables and Parameters*

Variables / Parameters	Description
$S(t)$	Number of susceptible humans at a time t
$E(t)$	Number of exposed humans at a time t
$Q(t)$	Number of quarantined humans at a time t
$I(t)$	Number of infected humans at a time t
$J(t)$	Number of isolated humans at a time t
$R(t)$	Number of recovered humans at a time t
N	Total human population
Π	Rate of recruitment (from birth and immigration)
μ	Rate of natural mortality
β	Rate of effective contacts resulting to disease transmission among humans
ε_1, ε_2	Rates of infectivity reduction in quarantined and isolated sub-populations respectively due to hygiene precautions
η $(0 \le \eta \le 1)$	Rate of social distancing
τ_1, τ_2	Rates of contact tracing for the exposed and infected sub-populations respectively
δ_1, δ_2 $(\delta_1 > \delta_2)$	Rates of COVID-19 related mortality for infected and isolated sub-populations respectively
ρ	Rate of progression from the exposed sub-population
θ $(0 \le \theta \le 1)$	Proportion of exposed individuals who are identified and quarantined
σ	Rate of progression from the quarantined sub-population
ξ $(0 \le \xi \le 1)$	Proportion of quarantined individuals who are confirmed COVID-19 positive and are isolated
γ_1	Rate of progression from the infected sub-population
φ $(0 \le \varphi \le 1)$	Rate of isolation of the infected individuals
$(1-\varphi)$	Proportion of infected individuals who recover
γ_2	Rate of recovery of isolated individuals due to supportive/symptoms treatment
κ	Rate of reinfection (Immunity loss rate) of the recovered individuals

Now to normalize the populations, set

$$s(t)=\frac{S(t)}{N};\ e(t)=\frac{E(t)}{N};\ q(t)=\frac{Q(t)}{N};\ i(t)=\frac{I(t)}{N};\ j(t)=\frac{J(t)}{N};\ r(t)=\frac{R(t)}{N} \quad (4)$$

where N is a constant, so that the dimensionless system in terms of the new variables with proportion is

$$\begin{aligned}
\frac{ds(t)}{dt} &= \Pi-\mu s(t)-(1-\eta)\beta\left(\varepsilon_1 q(t)+i(t)+\varepsilon_1 j(t)\right)s(t)+(1-\xi)\sigma q(t)+\kappa r(t)\\
\frac{de(t)}{dt} &= (1-\eta)\beta\left(\varepsilon_1 q(t)+i(t)+\varepsilon_1 j(t)\right)s(t)-(\mu+\tau_1+\rho)e(t)\\
\frac{dq(t)}{dt} &= (\theta\rho+\tau_1)e(t)-(\mu+\sigma)q(t)\\
\frac{di(t)}{dt} &= (1-\theta)\rho e(t)-(\mu+\delta_1+\tau_2+\gamma_1)i(t) \qquad (5)\\
\frac{dj(t)}{dt} &= \xi\sigma q(t)+(\tau_2+\varphi\gamma_1)i(t)-(\mu+\delta_2+\gamma_2)j(t)\\
\frac{dr(t)}{dt} &= (1-\varphi)\gamma_1 i(t)+\gamma_2 j(t)-(\mu+\kappa)r(t);
\end{aligned}$$

where $N=s(t)+e(t)+q(t)+i(t)+j(t)+r(t)=1,$ (6)

with initial conditions:

$$s(0)=s_0,\ e(0)=e_0,\ q(0)=q_0,\ i(0)=i_0,\ j(0)=j_0,\ r(0)=r_0. \quad (7)$$

C. Positivity and Boundedness of Solutions

Since the system under consideration involves population, it is important to establish that it is biologically feasible. This is done by showing that all solutions to the model equations are non-negative at any time t.

***Theorem* 1:** Let the initial conditions of the state variables be such that

$\{s(0)\geq 0,\ e(0)\geq 0,\ q(0)\geq 0,\ i(0)\geq 0,\ j(0)\geq 0,\ r(0)\geq 0 \text{ and } N(0)\geq 0\}\in\Omega.$

Then the solution set $\{s(t),\ e(t),\ q(t),\ i(t),\ j(t),\ r(t) \text{ and } N(t)\}$ is non-negative in Ω for all time $t\geq 0$.

Proof: Each equation in the normalized model (5) is considered for the positivity of the state variables as follows.

$$\frac{ds(t)}{dt}=\Pi-\mu s(t)-(1-\eta)\beta\left(\varepsilon_1 q(t)+i(t)+\varepsilon_1 j(t)\right)s(t)+(1-\xi)\sigma q(t)+\kappa r(t)$$

$$\Rightarrow \frac{ds(t)}{dt}\geq -\left[\mu+(1-\eta)\beta\left(\varepsilon_1 q(t)+i(t)+\varepsilon_1 j(t)\right)\right]s(t).$$

Separating the variables and integrating,

$$\int\frac{ds(t)}{s(t)}\geq -\int\left[\mu+(1-\eta)\beta\left(\varepsilon_1 q(t)+i(t)+\varepsilon_1 j(t)\right)\right]dt$$

$$\Rightarrow \ln s(t)\geq -\left[\mu+(1-\eta)\beta\left(\varepsilon_1 q(t)+i(t)+\varepsilon_1 j(t)\right)\right]t+c_1,$$

where c_1 is a constant of integration.

Then $s(t)\geq s_0 e^{-\left[\mu+(1-\eta)\beta(\varepsilon_1 q(t)+i(t)+\varepsilon_1 j(t))\right]t}$, where $s_0:=e^{c_1}$.

$\Rightarrow \quad s(t)\geq 0,\ \forall\ t\geq 0 \qquad$ (since $s_0\geq 0$).

Other state variables can also be shown to be non-negative in a similar manner. Hence, all the state variables are non-negative in the region Ω for all time $t\geq 0$, whenever the initial values are non-negative.

***Theorem* 2:** Every solution in the solution set $\{s(t),\ e(t),\ q(t),\ i(t),\ j(t),\ r(t) \text{ and } N(t)\}$ for the normalized model equation (5) is attracting.

This implies that every solution approaches and remains in the region Ω as $t\to\infty$.

***Proof*:** Recall that

$$\begin{aligned}
N &= s(t)+e(t)+q(t)+i(t)+j(t)+r(t)\\
\frac{dN}{dt} &= \frac{ds(t)}{dt}+\frac{de(t)}{dt}+\frac{dq(t)}{dt}+\frac{di(t)}{dt}+\frac{dj(t)}{dt}+\frac{dr(t)}{dt}\\
&= \Pi-\mu\left(s(t)+e(t)+q(t)+i(t)+j(t)+r(t)\right)-\left(\delta_1 i(t)+\delta_2 j(t)\right)\\
&= \Pi-\mu N-\left(\delta_1 i(t)+\delta_2 j(t)\right).
\end{aligned}$$

$$\Rightarrow \frac{dN}{dt}\leq \Pi-\mu N.$$

Separating the variables and integrating,

$$\int\frac{dN}{\Pi-\mu N}\leq\int dt$$

$$\Rightarrow \quad -\frac{1}{\mu}\ln\left(\Pi-\mu N\right)\leq t+c, \text{ where } c \text{ is a constant.}$$

$$\Rightarrow \quad \ln\left(\Pi-\mu N\right)\geq -\mu t+C, \text{ where } C=-\mu c.$$

$$\Rightarrow \quad \Pi-\mu N\geq Ae^{-\mu t}, \text{ where } A=e^{-\mu c}.$$

Thus $\quad N(t)\leq\frac{\Pi}{\mu}-\frac{A}{\mu}e^{-\mu t}$

$$t=0\Rightarrow N(0)\leq\frac{\Pi}{\mu}-\frac{A}{\mu}=\frac{\Pi-A}{\mu}=N_0$$

$$\Rightarrow A=\Pi-\mu N_0$$

Thus $\quad N(t)\leq\frac{\Pi}{\mu}-\left(\frac{\Pi-\mu N_0}{\mu}\right)e^{-\mu t}$

As $t\to 0,\ N(t)\to\frac{\Pi}{\mu}$ $\qquad \left(\text{i.e. } N(t)\leq\frac{\Pi}{\mu}=1, \text{ for large } t\right).$

Thus every solution with initial conditions in $\mathbb{R}^6_+$ approaches and remains in that region for all $t\geq 0$; and so the region is positively invariant.

This result together with that of Theorem 1 implies that

$$\Omega=\left\{\left(s(t),\ e(t),\ q(t),\ i(t),\ j(t),\ r(t)\right)\in\mathbb{R}^6_+ : N(t)\leq\frac{\Pi}{\mu}\right\}$$

$0 \le N(t) \le \dfrac{\Pi}{\mu}$ $\left(\text{or } 0 \le N(t) \le 1, \text{ since } N=1\right)$ at any time $t \ge 0$.

i.e. the model solutions are positive and bounded at any time *t*, and so it is both epidemiologically feasible and mathematically

$$\frac{ds(t)}{dt} = \frac{de(t)}{dt} = \frac{dq(t)}{dt} = \frac{di(t)}{dt} = \frac{dj(t)}{dt} = \frac{dr(t)}{dt} = 0. \qquad (8)$$

well posed. Hence, it is sufficient to study the dynamics of the model in the region Ω.

III. MATHEMATICAL ANALYSIS OF THE MODEL

In this section we carry out qualitative analysis of the model (5) to investigate existence and stability of the steady states. At steady states,

The steady state system of the model equation (5) is given as

$$\begin{aligned}
0 &= \Pi - \mu s^*(t) - (1-\eta)\beta\left(\varepsilon_1 q^*(t) + i^*(t) + \varepsilon_1 j^*(t)\right)s^*(t) + (1-\xi)\sigma q^*(t) + \kappa r^*(t)\\
0 &= (1-\eta)\beta\left(\varepsilon_1 q^*(t) + i^*(t) + \varepsilon_1 j^*(t)\right)s^*(t) - (\mu + \tau_1 + \rho)e^*(t)\\
0 &= (\theta\rho + \tau_1)e^*(t) - (\mu + \sigma)q^*(t) \qquad (9)\\
0 &= (1-\theta)\rho e^*(t) - (\mu + \delta_1 + \tau_2 + \gamma_1)i^*(t)\\
0 &= \xi\sigma q^*(t) + (\tau_2 + \varphi\gamma_1)i^*(t) - (\mu + \delta_2 + \gamma_2)j^*(t)\\
0 &= (1-\varphi)\gamma_1 i^*(t) + \gamma_2 j^*(t) - (\mu + \kappa)r^*(t);
\end{aligned}$$

The model exhibits two equilibria depending on whether or not there is COVID-19 in the population.

A. *Existence and Stability of Disease-free Equilibrium, E_0*

Disease-free equilibrium points are steady-state solutions of the model equations when COVID-19 is absent in the population. This corresponds to the solution of the system (9) when $e^*(t) = q^*(t) = i^*(t) = j^*(t) = 0$. Thus the disease-free equilibrium of the model is obtained as

$$E_0 = \left(\frac{\Pi}{\mu}, 0, 0, 0, 0, 0\right),$$

or equivalently, $E_0 = (1, 0, 0, 0, 0, 0)$ (10)

- *Computation of the Basic Reproduction Number, R_0*

To compute the Basic Reproduction Number (R_0) of the model, the next generation matrix approach described by Driessche and Watmough [27] is employed. Using this approach, R_0 is defined as the spectra radius (dominant eigenvalue) of the Next Generation Operator, FV^{-1} [28]. i.e.

$$R_0 = \rho\left(FV^{-1}\right), \qquad (11)$$

where F and V are the respective Jacobian matrices of the transmission and transition matrices evaluated at E_0. These are defined as

$$F = \begin{pmatrix} 0 & (1-\eta)\beta\varepsilon_1 & (1-\eta)\beta & (1-\eta)\beta\varepsilon_2 \\ 0 & 0 & 0 & 0 \\ 0 & 0 & 0 & 0 \\ 0 & 0 & 0 & 0 \end{pmatrix} \text{ and } V = \begin{pmatrix} \mu+\tau_1+\rho & 0 & 0 & 0 \\ -(\theta\rho+\tau_1) & \mu+\sigma & 0 & 0 \\ -(1-\theta)\rho & 0 & \mu+\delta_1+\tau_2+\gamma_1 & 0 \\ 0 & -\xi\sigma & -(\tau_2+\varphi\gamma_1) & \mu+\delta_2+\gamma_2 \end{pmatrix}$$

Now, FV^{-1} has the characteristics equation given as

$$\begin{vmatrix} \dfrac{(1-\eta)\beta}{\mu+\tau_1+\rho}\{\varepsilon_1 R_1 + R_2 + \varepsilon_2 R_3\} - \lambda & \dfrac{(1-\eta)\beta\varepsilon_1}{\mu+\sigma} & \dfrac{(1-\eta)\beta}{(\mu+\delta_1+\tau_2+\gamma_1)}\left[1 + \dfrac{\varepsilon_2(\tau_2+\varphi\gamma_1)}{\mu+\delta_2+\gamma_2}\right] & \dfrac{(1-\eta)\beta\varepsilon_2}{\mu+\delta_2+\gamma_2} \\ 0 & -\lambda & 0 & 0 \\ 0 & 0 & -\lambda & 0 \\ 0 & 0 & 0 & -\lambda \end{vmatrix} = 0$$

$$\Rightarrow \left\{\frac{(1-\eta)\beta}{\mu+\tau_1+\rho}\left[\varepsilon_1 R_1 + R_2 + \varepsilon_2 R_3\right] - \lambda\right\}(-\lambda)^3 = 0$$

$$\Rightarrow \lambda = 0 \text{ (thrice)}, \quad \text{or} \quad \lambda = \frac{(1-\eta)\beta}{\mu+\tau_1+\rho}\left[\varepsilon_1 R_1 + R_2 + \varepsilon_2 R_3\right] = R_0 \qquad (12)$$

where $R_1 = \dfrac{(\theta\rho+\tau_1)}{\mu+\sigma}$, $R_2 = \dfrac{(1-\theta)\rho}{\mu+\delta_1+\tau_2+\gamma_1}$ and $R_3 = \dfrac{(\mu+\delta_1+\tau_2+\gamma_1)(\theta\rho+\tau_1)\xi\sigma + (\mu+\sigma)(\tau_2+\varphi\gamma_1)(1-\theta)\rho}{(\mu+\sigma)(\mu+\delta_1+\tau_2+\gamma_1)(\mu+\delta_2+\gamma_2)}$. (13)

Hence,

$$R_0 = \frac{(1-\eta)\beta}{\mu+\tau_1+\rho}\left\{\frac{\varepsilon_1(\theta\rho+\tau_1)}{\mu+\sigma} + \frac{(1-\theta)\rho}{\mu+\delta_1+\tau_2+\gamma_1} + \frac{\varepsilon_2\left[(\mu+\delta_1+\tau_2+\gamma_1)(\theta\rho+\tau_1)\xi\sigma + (\mu+\sigma)(\tau_2+\varphi\gamma_1)(1-\theta)\rho\right]}{(\mu+\sigma)(\mu+\delta_1+\tau_2+\gamma_1)(\mu+\delta_2+\gamma_2)}\right\} \qquad (14)$$

This quantity gives the reproduction number, which is an important notion in epidemiology. It is a threshold value that is often used to measure the spread of a disease. It is defined as the average number of secondary cases produced by a "typical" infected (assumed infectious) individual during his/her entire life as infectious (infectious period) when introduced in a fully susceptible population [29].

The above quantity in (3.6) can be referred to as the control reproduction number, since the model from which it was obtained incorporates control parameters. In the absence of all the controls, the above reproduction in (3.6) becomes

$$\Re_0 = \frac{\beta\rho}{(\mu+\rho)(\mu+\delta_1+\gamma_1)}. \qquad (15)$$

➢ *Local Stability of the Disease-free Equilibrium*

***Theorem* 3:** If $R_0 < 1$, and if $\frac{(1-\eta)\beta}{\mu+\tau_1+\rho}\left[\varepsilon_1 R_1 + R_2\right] < 1 + A_1$ and $\frac{(1-\eta)\beta}{\mu+\tau_1+\rho}\left[\varepsilon_1 R_1 + A_3\right] < 1 + A_2$, then the disease-free equilibrium is locally asymptotically stable. Otherwise, it is unstable.

Proof: The local stability of the disease-free equilibrium is determined by the eigenvalue of the Jacobian matrix of the system (5), evaluated at E_0, thus;

$$J\big|_{E_0} = \begin{pmatrix} -\mu & 0 & -(1-\eta)\beta\varepsilon_1 + (1-\xi)\sigma & -(1-\eta)\beta & -(1-\eta)\beta\varepsilon_2 & \kappa \\ 0 & -(\mu+\tau_1+\rho) & (1-\eta)\beta\varepsilon_1 & (1-\eta)\beta & (1-\eta)\beta\varepsilon_2 & 0 \\ 0 & \theta\rho+\tau_1 & -(\mu+\sigma) & 0 & 0 & 0 \\ 0 & (1-\theta)\rho & 0 & -(\mu+\delta_1+\tau_2+\gamma_1) & 0 & 0 \\ 0 & 0 & \xi\sigma & \tau_2+\varphi\gamma_1 & -(\mu+\delta_2+\gamma_2) & 0 \\ 0 & 0 & 0 & (1-\varphi)\gamma_1 & \gamma_2 & -(\mu+\kappa) \end{pmatrix}$$

Matrix J has eigenvalues $\lambda = -\mu$ and $\lambda = -(\mu+\kappa)$; others being the roots of the quartic equation:

$$\begin{aligned} &\lambda^4 + \left[(\mu+\tau_1+\rho)+(\mu+\sigma)+(\mu+\delta_1+\tau_2+\gamma_1)+(\mu+\delta_2+\gamma_2)\right]\lambda^3 + (\mu+\tau_1+\rho)(\mu+\sigma)\left\{(1+A_1) - \frac{(1-\eta)\beta}{\mu+\tau_1+\rho}\left[\varepsilon_1 R_1 + R_2\right]\right\}\lambda^2 \\ &+ (\mu+\tau_1+\rho)(\mu+\sigma)\left[(\mu+\delta_1+\tau_2+\gamma_1)+(\mu+\delta_2+\gamma_2)\right]\left\{(1+A_2) - \frac{(1-\eta)\beta}{\mu+\tau_1+\rho}\left[\varepsilon_1 R_1 + A_3\right]\right\}\lambda \qquad (16) \\ &+ (\mu+\tau_1+\rho)(\mu+\sigma)(\mu+\delta_1+\tau_2+\gamma_1)(\mu+\delta_2+\gamma_2)\left[1-R_0\right] = 0; \end{aligned}$$

where $A_1 = \frac{\left[(\mu+\tau_1+\rho)+(\mu+\sigma)\right]\left[(\mu+\delta_1+\tau_2+\gamma_1)+(\mu+\delta_2+\gamma_2)\right] + (\mu+\delta_1+\tau_2+\gamma_1)(\mu+\delta_2+\gamma_2)}{(\mu+\tau_1+\rho)(\mu+\sigma)}$,

$$A_2 = \frac{\left[(\mu+\tau_1+\rho)+(\mu+\sigma)\right](\mu+\delta_1+\tau_2+\gamma_1)(\mu+\delta_2+\gamma_2)}{(\mu+\tau_1+\rho)(\mu+\sigma)\left[(\mu+\delta_1+\tau_2+\gamma_1)+(\mu+\delta_2+\gamma_2)\right]}, \qquad (17)$$

$$A_3 = \frac{\left[(\mu+\sigma)+(\mu+\delta_2+\gamma_2)\right](1-\theta)\rho + \varepsilon_1\left[(\theta\rho+\tau_1)\xi\sigma + (\tau_2+\varphi\gamma_1)(1-\theta)\rho\right]}{(\mu+\sigma)\left[(\mu+\delta_1+\tau_2+\gamma_1)+(\mu+\delta_2+\gamma_2)\right]}$$

with R_0 as defined in (14) and R_1, R_2 as defined in (13).

Now, if $R_0 < 1$, and if $\frac{(1-\eta)\beta}{\mu+\tau_1+\rho}\left[\varepsilon_1 R_1 + R_2\right] < 1 + A_1$ and $\frac{(1-\eta)\beta}{\mu+\tau_1+\rho}\left[\varepsilon_1 R_1 + A_3\right] < 1 + A_2$, then by Descartes' rule of signs, the roots of the quartic equation (16) are negative (or complex with negative real parts). Hence, the disease-free equilibrium is locally asymptotically stable. Otherwise, it is unstable.

➢ *Global Stability of the Disease-free Equilibrium*

The global stability analysis of the disease-free equilibrium for the COVID-19 model is explored using the Next Generation Operator method described by Castillo-Chavez *et al*. [30]. This is done as follows.

Considering the model equations (5), the system of equations can be rewritten in the form:

$$\begin{aligned} \frac{dX}{dt} &= F(X,Y) \\ \frac{dY}{dt} &= G(X,Y),\ G(X,0) = 0; \end{aligned} \qquad (18)$$

where $X \in \mathbb{R}^m$ denotes (its components) the number of uninfected individuals and $Y \in \mathbb{R}^n$ denotes (its components) the number of infected individuals, including the latent and infectious ones; $E_0 = (x^*, 0)$ denotes the disease-free equilibrium of the system.

***Theorem* 4:** The disease-free equilibrium, $E_0 = (1, 0, 0, 0, 0, 0)$, of the system is globally asymptotically stable (GAS) provided

that $R_0 < 1$ (i.e. if it is locally asymptotically stable) and the assumptions ($H1$) and ($H2$) below hold:

$H1$: For $\frac{dX}{dt} = F(X,0)$, X^* is GAS;

$H2$: $G(X,Y) = AY - \hat{G}(X,Y)$, $\hat{G}(X,Y) \geq 0$ for $(X,Y) \in \Omega$,

where $A = D_Y G(X^*,0)$ is a Metzler-matrix (the off diagonal elements of A are non-negative) and Ω is the region where the model is biologically feasible.

From the model equation (2.5), $X = (s, r)$ and $Y = (e, q, i, j)$ so that $F(X, 0) = \begin{pmatrix} \Pi - \mu s(t) \\ 0 \end{pmatrix}$,

$$A = D_Y(X^*,0) = \begin{pmatrix} -(\mu+\tau_1+\rho) & (1-\eta)\beta\varepsilon_1 & (1-\eta)\beta & (1-\eta)\beta\varepsilon_2 \\ \theta\rho+\tau_1 & -(\mu+\sigma) & 0 & 0 \\ (1-\theta)\rho & 0 & -(\mu+\delta_1+\tau_2+\gamma_1) & 0 \\ 0 & \xi\sigma & \tau_2+\varphi\gamma_1 & -(\mu+\delta_2+\gamma_2) \end{pmatrix}$$

and

$$G(X,Y) = \begin{pmatrix} (1-\eta)\beta(\varepsilon_1 q(t) + i(t) + \varepsilon_1 j(t))s(t) - (\mu+\tau_1+\rho)e(t) \\ (\theta\rho+\tau_1)e(t) - (\mu+\sigma)q(t) \\ (1-\theta)\rho e(t) - (\mu+\delta_1+\tau_2+\gamma_1)i(t) \\ \xi\sigma q(t) + (\tau_2+\varphi\gamma_1)i(t) - (\mu+\delta_2+\gamma_2)j(t) \end{pmatrix}.$$

Then $G(X,Y) = AY - \hat{G}(X,Y) \Rightarrow \hat{G}(X,Y) = AY - G(X,Y)$.

$$\hat{G}(X,Y) = A\begin{pmatrix} e(t) \\ q(t) \\ i(t) \\ j(t) \end{pmatrix} - G(X,Y)$$

$$= \begin{pmatrix} (1-\eta)\beta(\varepsilon_1 q(t) + i(t) + \varepsilon_1 j(t)) - (\mu+\tau_1+\rho)e(t) \\ (\theta\rho+\tau_1)e(t) - (\mu+\sigma)q(t) \\ (1-\theta)\rho e(t) - (\mu+\delta_1+\tau_2+\gamma_1)i(t) \\ \xi\sigma q(t) + (\tau_2+\varphi\gamma_1)i(t) - (\mu+\delta_2+\gamma_2)j(t) \end{pmatrix} - G(X,Y)$$

$$= \begin{pmatrix} (1-\eta)\beta(\varepsilon_1 q(t) + i(t) + \varepsilon_1 j(t))[1-s(t)] \\ 0 \\ 0 \\ 0 \end{pmatrix} = \begin{pmatrix} \hat{G}_1(X,Y) \\ \hat{G}_2(X,Y) \\ \hat{G}_3(X,Y) \\ \hat{G}_4(X,Y) \end{pmatrix}.$$

Obviously, $\hat{G}_2(X,Y) = \hat{G}_3(X,Y) = \hat{G}_4(X,Y) = 0$; and $\hat{G}_1(X,Y) \geq 0$, since $0 \leq s(t) \leq 1$ at any time t.

Now, it has been established that

(i) $X^* = (1, 0)$ is a GAS equilibrium of $\frac{dX}{dt} = F(X,0)$; and

(ii) $\hat{G}(X,Y) \geq 0$, for $(X,Y) \in \Omega$.

Hence, the disease-free equilibrium, $E_0 = (1, 0, 0, 0, 0, 0)$, of the system is globally asymptotically stable when $R_0 < 1$. Otherwise, it is unstable. This completes the proof.

B. Existence and Stability of Endemic Equilibrium, E^e

The endemic equilibrium points are steady-state solutions of the model equations when COVID-19 is present in the population. This corresponds to the solution of the system (9) when $e^*(t) \neq q^*(t) \neq i^*(t) \neq j^*(t) \neq 0$. Thus the endemic equilibrium, E^e, of the model is obtained as:

$$E^e = (s^*(t), e^*(t), q^*(t), i^*(t), j^*(t), r^*(t)) \quad (19)$$

where

$$s^*(t) = \frac{\Pi}{\mu} - \frac{1}{\mu}\left\{1 - \left[(1-\xi)\sigma R_1 + \frac{\kappa}{\mu+\kappa}\left((1-\varphi)\gamma_1 R_2 + \gamma_2 R_3\right)\right]\right\}e^*(t)$$

$$q^*(t) = \frac{\theta\rho+\tau_1}{\mu+\sigma}e^*(t)$$

$$i^*(t) = \frac{(1-\theta)\rho}{\mu+\delta_1+\tau_2+\gamma_1}e^*(t)$$

$$j^*(t) = \frac{(\mu+\delta_1+\tau_2+\gamma_1)(\theta\rho+\tau_1)\xi\sigma + (\mu+\sigma)(\tau_2+\varphi\gamma_1)(1-\theta)\rho}{(\mu+\sigma)(\mu+\delta_1+\tau_2+\gamma_1)(\mu+\delta_2+\gamma_2)}e^*(t)$$

$$r^*(t) = \frac{e^*(t)}{\mu+\kappa}\left[(1-\varphi)\gamma_1 R_2 + \gamma_2 R_3\right]$$

and $e^*(t) = \dfrac{\mu(R_0-1)}{R_0\left\{1 - \left[(1-\xi)\sigma R_1 + \frac{\kappa}{\mu+\kappa}\left((1-\varphi)\gamma_1 R_2 + \gamma_2 R_3\right)\right]\right\}}$

with R_1, R_2 and R_3 as defined in (13) and R_0 as defined in (14). Hence, the endemic equilibrium, E^e, exists for the system only if $R_0 > 1$ and $\left[(1-\xi)\sigma R_1 + \frac{\kappa}{\mu+\kappa}\left((1-\varphi)\gamma_1 R_2 + \gamma_2 R_3\right)\right]$ is less than unity, and no endemic equilibrium exists if otherwise.

It is remarkable to note that if $R_0 = 1$, then the endemic equilibrium coincides with the disease-free equilibrium.

➢ *Local stability of the Endemic Equilibrium*

***Theorem* 5:** If $R_0 > 1$, there exists an endemic equilibrium, which is locally asymptotically stable iff for constants a_i, $i = 1, 2...10$, $a_1 > a_2$; $a_3 > a_4$; $a_5 > a_6$; $a_7 > a_8$; $a_9 > a_{10}$. Otherwise, it is unstable.

Proof: The local stability of the endemic equilibrium is determined by the eigenvalue of the Jacobian matrix of the system (5), evaluated at E^e, thus;

ISSN No:-2456-2165

$$J\Big|_{E^e}=\begin{pmatrix} -\left(\mu+R_0e^*(t)\right) & 0 & -\dfrac{(1-\eta)\beta\varepsilon_1}{R_0}+(1-\xi)\sigma & -\dfrac{(1-\eta)\beta}{R_0} & -\dfrac{(1-\eta)\beta\varepsilon_2}{R_0} & \kappa \\ R_0e^*(t) & -(\mu+\tau_1+\rho) & \dfrac{(1-\eta)\beta\varepsilon_1}{R_0} & \dfrac{(1-\eta)\beta}{R_0} & \dfrac{(1-\eta)\beta\varepsilon_2}{R_0} & 0 \\ 0 & \theta\rho+\tau_1 & -(\mu+\sigma) & 0 & 0 & 0 \\ 0 & (1-\theta)\rho & 0 & -(\mu+\delta_1+\tau_2+\gamma_1) & 0 & 0 \\ 0 & 0 & \xi\sigma & \tau_2+\varphi\gamma_1 & -(\mu+\delta_2+\gamma_2) & 0 \\ 0 & 0 & 0 & (1-\varphi)\gamma_1 & \gamma_2 & -(\mu+\kappa) \end{pmatrix}$$

Matrix J has eigenvalues being the roots of the polynomial equation:

$$\lambda^6+(c_1+c_2+c_3+c_4+c_5+c_6)\lambda^5+(a_1-a_2)\lambda^4+(a_3-a_4)\lambda^3+(a_5-a_6)\lambda^2+(a_7-a_8)\lambda+(a_9-a_{10})=0, \quad (20)$$

where

$$c_1=\left(\mu+R_0e^*(t)\right);\ c_2=(\mu+\tau_1+\rho);\ c_3=(\mu+\sigma);\ c_4=(\mu+\delta_1+\tau_2+\gamma_1);\ c_5=(\mu+\delta_2+\gamma_2);\ c_6=(\mu+\kappa),$$

and

$$a_1=c_1c_2+c_3c_4+c_5c_6+(c_1+c_2)(c_3+c_4)+(c_1+c_2)(c_5+c_6)+(c_3+c_4)(c_5+c_6);$$

$$a_2=\frac{(1-\eta)\beta}{R_0}\left[\varepsilon_1(\theta\rho+\tau_1)+(1-\theta)\rho\right];$$

$$a_3=c_1c_2(c_3+c_4)+c_1c_2(c_5+c_6)+c_3c_4(c_5+c_6)+(c_1+c_2)c_3c_4+(c_1+c_2)c_5c_6+(c_3+c_4)c_5c_6$$
$$+(c_1+c_2)(c_3+c_4)(c_5+c_6)+\left[\frac{(1-\eta)\beta\varepsilon_1}{R_0}-(1-\xi)\sigma\right](\theta\rho+\tau_1)R_0e^*(t)+(1-\eta)\beta(1-\theta)\rho e^*(t);$$

$$a_4=\frac{(1-\eta)\beta}{R_0}\left\{\varepsilon_1(\theta\rho+\tau_1)(c_1+c_2+c_3+c_4)+(1-\theta)\rho(c_1+c_3+c_5+c_6)+\varepsilon_2\left[(\theta\rho+\tau_1)\xi\sigma+(\tau_2+\varphi\gamma_1)(1-\theta)\rho\right]\right\};$$

$$a_5=c_1c_2c_3c_4+c_1c_2c_5c_6+c_3c_4c_5c_6+c_1c_2(c_3+c_4)(c_5+c_6)+c_3c_4(c_1+c_2)(c_5+c_6)+(c_1+c_2)(c_3+c_4)c_5+c_6$$
$$+\left[\frac{(1-\eta)\beta\varepsilon_1}{R_0}-(1-\xi)\sigma\right](\theta\rho+\tau_1)R_0e^*(t)(c_4+c_5+c_6)+(1-\eta)\beta e^*(t)\left\{\begin{matrix}(1-\theta)\rho(c_3+c_5+c_6)+\\ \varepsilon_2\left[(\theta\rho+\tau_1)\xi\sigma+(\tau_2+\varphi\gamma_1)(1-\theta)\rho\right]\end{matrix}\right\};$$

$$a_6=\frac{(1-\eta)\beta}{R_0}\left\{\begin{matrix}\varepsilon_1(\theta\rho+\tau_1)\left[c_1c_4+c_5c_6+(c_1+c_4)(c_5+c_6)\right]+(1-\theta)\rho\left[c_1c_3+c_5c_6+(c_1+c_3)(c_5+c_6)\right]\\ +\varepsilon_2\left[(\theta\rho+\tau_1)\xi\sigma(c_1+c_4+c_6)+(\tau_2+\varphi\gamma_1)(1-\theta)\rho(c_1+c_3+c_6)\right]+\kappa R_0e^*(t)(1-\theta)\rho(1-\varphi)\gamma_1\end{matrix}\right\};$$

$$a_7=c_1c_2c_3c_4(c_5+c_6)+c_1c_2c_5c_6(c_3+c_4)+(c_1+c_2)c_3c_4c_5c_6+\left[\frac{(1-\eta)\beta\varepsilon_1}{R_0}-(1-\xi)\sigma\right](\theta\rho+\tau_1)R_0e^*(t)(c_4+c_5)c_4c_5c_6$$
$$+(1-\eta)\beta e^*(t)\left\{(1-\theta)\rho(c_3+c_5)c_3c_5c_6+\varepsilon_2\left[(\theta\rho+\tau_1)\xi\sigma(c_4+c_6)+(\tau_2+\varphi\gamma_1)(1-\theta)\rho(c_3+c_6)\right]\right\};$$

$$a_8=\frac{(1-\eta)\beta}{R_0}\left\{\begin{matrix}\varepsilon_1(\theta\rho+\tau_1)\left[c_1c_4(c_5+c_6)+(c_1+c_4)c_5c_6\right]+(1-\theta)\rho\left[c_1c_3(c_5+c_6)+(c_1+c_3)c_5c_6\right]\\ +\varepsilon_2\left[(\theta\rho+\tau_1)\xi\sigma(c_1+c_4)c_1c_4c_6+(\tau_2+\varphi\gamma_1)(1-\theta)\rho(c_1+c_3)c_1c_3c_6\right]\end{matrix}\right\}$$
$$+\kappa R_0e^*(t)\left\{(1-\theta)\rho(1-\varphi)\gamma_1(c_3+c_5)+\gamma_2\left[(\theta\rho+\tau_1)\xi\sigma+(\tau_2+\varphi\gamma_1)(1-\theta)\rho\right]\right\};$$

$$a_9=c_1c_2c_3c_4c_5c_6+\left[\frac{(1-\eta)\beta\varepsilon_1}{R_0}-(1-\xi)\sigma\right](\theta\rho+\tau_1)R_0e^*(t)(c_4+c_5)c_4c_5c_6$$
$$+(1-\eta)\beta e^*(t)\left\{(1-\theta)\rho c_3c_5c_6+\varepsilon_2\left[(\theta\rho+\tau_1)\xi\sigma c_4c_6+(\tau_2+\varphi\gamma_1)(1-\theta)\rho c_3c_6\right]\right\};$$

$$a_{10}=\frac{(1-\eta)\beta}{R_0}\left\{\varepsilon_1(\theta\rho+\tau_1)(c_1c_2c_3c_4)+(1-\theta)\rho c_1c_3c_5c_6+\varepsilon_2\left[(\theta\rho+\tau_1)\xi\sigma c_1c_4c_6+(\tau_2+\varphi\gamma_1)(1-\theta)\rho c_1c_3c_6\right]\right\}$$
$$+\kappa R_0e^*(t)\left\{(1-\theta)\rho(1-\varphi)\gamma_1c_3c_5+\gamma_2\left[(\theta\rho+\tau_1)\xi\sigma c_4+(\tau_2+\varphi\gamma_1)(1-\theta)\rho c_3\right]\right\};$$

are positive constants.

Now, if $a_1 > a_2; a_3 > a_4; a_5 > a_6; a_7 > a_8; a_9 > a_{10}$, then by Descartes' rule of sign, the polynomial equation (20) has no sign change, and so all the roots are negative (or complex with negative real parts). Hence, the endemic equilibrium, E^e, is locally asymptotically stable.

➢ *Global Stability of the Endemic Equilibrium*

The global stability of the COVID-19 endemic equilibrium, E^e, is obtained by means of Lyapunov's direct method and the LaSalles's invariance principle [31,32].

***Theorem* 6:** Consider the normalized model equation (5) for COVID-19. Let $E^e = \left(s^*, e^*, q^*, i^*, j^*, r^*\right)$ be a critical solution (i.e. the endemic equilibrium points). If there exist a positive definite scalar function, $V_e\left(s^*, e^*, q^*, i^*, j^*, r^*\right)$ such that $\frac{dV_e}{dt} < 0$. Then $V_e\left(s^*, e^*, q^*, i^*, j^*, r^*\right)$ is a Lyapunov function for the system and E^e is globally asymptotically stable.

***Proof*:** Consider the nonlinear Lyapunov function

$$\begin{aligned} V_e &= \lambda\left(s - s^* - s^*\log\frac{s}{s^*}\right) + \lambda\left(e - e^* - e^*\log\frac{e}{e^*}\right) \\ &+ \lambda\left(q - q^* - q^*\log\frac{e}{q^*}\right) + \lambda\left(i - i^* - i^*\log\frac{i}{i^*}\right) \\ &+ \lambda\left(j - j^* - j^*\log\frac{j}{j^*}\right) + \lambda\left(r - r^* - r^*\log\frac{r}{r^*}\right), \end{aligned} \tag{21}$$

where V_e is $C^{'}$ (compact) in the interior of the region Ω. E^e is the global minimum of V_e on the region Ω and $V_e\left(s^*, e^*, q^*, i^*, j^*, r^*\right) \geq 0$. The time derivative of V_e defined in equation (21) is obtained thus:

$$\begin{aligned} \dot{V}_e = \frac{dV_e}{dt} &= \lambda\left(1 - \frac{s^*}{s}\right)\frac{ds}{dt} + \lambda\left(1 - \frac{e^*}{e}\right)\frac{de}{dt} + \lambda\left(1 - \frac{q^*}{q}\right)\frac{dq}{dt} \\ &+ \lambda\left(1 - \frac{i^*}{i}\right)\frac{di}{dt} + \lambda\left(1 - \frac{j^*}{j}\right)\frac{dj}{dt} + \lambda\left(1 - \frac{r^*}{r}\right)\frac{dr}{dt} \\ &= \lambda\left(\frac{S - s^*}{S}\right)\left[\begin{matrix} \Pi - \mu s(t) - (1-\eta)\beta\left(\varepsilon_1 q(t) + i(t) + \varepsilon_1 j(t)\right)s(t) \\ + (1-\xi)\sigma q(t) + \kappa r(t) \end{matrix}\right] \\ &+ \lambda\left(\frac{e - e^*}{e}\right)\left[(1-\eta)\beta\left(\varepsilon_1 q(t) + i(t) + \varepsilon_1 j(t)\right)s(t) - (\mu + \tau_1 + \rho)e(t)\right] \\ &+ \lambda\left(\frac{q - q^*}{q}\right)\left[(\theta\rho + \tau_1)e(t) - (\mu + \sigma)q(t)\right] \\ &+ \lambda\left(\frac{i - i^*}{i}\right)\left[(1-\theta)\rho e(t) - (\mu + \delta_1 + \tau_2 + \gamma_1)i(t)\right] \\ &+ \lambda\left(\frac{j - j^*}{j}\right)\left[\xi\sigma q(t) + (\tau_2 + \varphi\gamma_1)i(t) - (\mu + \delta_2 + \gamma_2)j(t)\right] \\ &+ \lambda\left(\frac{r - r^*}{r}\right)\left[(1-\varphi)\gamma_1 i(t) + \gamma_2 j(t) - (\mu + \kappa)r(t)\right]. \end{aligned}$$

At equilibrium, the time derivative for each class equals zero, implying from (9) that

$$\begin{aligned} &\Pi + (1-\xi)\sigma q(t) + \kappa r(t) = \left[\mu + (1-\eta)\beta\left(\varepsilon_1 q(t) + i(t) + \varepsilon_1 j(t)\right)\right]s^*(t); \\ &(1-\eta)\beta\left(\varepsilon_1 q(t) + i(t) + \varepsilon_1 j(t)\right)s(t) = (\mu + \tau_1 + \rho)e^*(t); \\ &(\theta\rho + \tau_1)e(t) = (\mu + \sigma)q^*(t);\ (1-\theta)\rho e(t) = (\mu + \delta_1 + \tau_2 + \gamma_1)i^*(t); \\ &\xi\sigma q(t) + (\tau_2 + \varphi\gamma_1)i(t) = (\mu + \delta_2 + \gamma_2)j^*(t); \\ &(1-\varphi)\gamma_1 i(t) + \gamma_2 j(t) = (\mu + \kappa)r^*(t); \end{aligned} \tag{22}$$

Putting (22) into $\dot{V}_e$ gives

$$\begin{aligned} \dot{V}_e = -\lambda\Bigg\{&\left(\frac{S - s^*}{S}\right)\left[\mu + (1-\eta)\beta\left(\varepsilon_1 q(t) + i(t) + \varepsilon_1 j(t)\right)\right]\left(s - s^*\right) \\ &+ \left(\frac{e - e^*}{e}\right)(\mu + \tau_1 + \rho)\left(e - e^*\right) + \left(\frac{q - q^*}{q}\right)(\mu + \sigma)\left(q - q^*\right) \\ &+ \left(\frac{i - i^*}{i}\right)(\mu + \delta_1 + \tau_2 + \gamma_1)\left(i - i^*\right) \\ &+ \left(\frac{j - j^*}{j}\right)(\mu + \delta_2 + \gamma_2)\left(j - j^*\right) + \left(\frac{r - r^*}{r}\right)(\mu + \kappa)\left(r - r^*\right)\Bigg\}. \end{aligned} \tag{23}$$

Now, the endemic equilibrium, $E^e = \left(s^*, e^*, q^*, i^*, j^*, r^*\right)$, being the global minimum of V_e implies that $s^* \leq s, e^* \leq e, q^* \leq q, i^* \leq i, j^* \leq j, r^* \leq r$. Therefore from (23), $\dot{V}_e < 0$. $\dot{V}_e = 0$ iff $s^* = s, e^* = e, q^* = q, i^* = i, j^* = j, r^* = r$. Thus the largest compact invariant set in $\left(s^*, e^*, q^*, i^*, j^*, r^*\right) \in \Omega : \dot{V}_e = 0$ is the singleton set E^e, which is the endemic equilibrium for the COVID-19 model. Hence, $E^e = \left(s^*, e^*, q^*, i^*, j^*, r^*\right)$ is globally asymptotically stable in the region Ω. This completes the proof.

IV. SENSITIVITY ANALYSIS AND NUMERICAL SIMULATIONS

A. *Sensitivity Analysis of R_0*

Sensitivity Analysis is an important notion in epidemiology, which determines the importance of each parameter to disease transmission. It is commonly used in determining the responsiveness of model prediction to parameter values, since there are usually errors in data collection and presumed parameter values. It is used to determine parameters that have high impact on the R_0 and which should be targeted by intervention strategies.

Parameters	Baseline Values	Sensitivity indices
μ	0.00000301	– 0.0000453431
η	0.25	– 1.0000000010
β	$0.62\text{x}10^{-8}$	+ 1.0000000000
ε_1	0.001	+ 0.0000338266
ε_2	0.00101	+ 0.0000448056
τ_1	0.06	– 0.2957380241
τ_2	0.07	– 0.2229445574
δ_1	0.01	– 0.1013426591
δ_2	0.001	– 0.0000001874
ρ	$1/7$	+ 0.2957528622
θ	0.3	– 0.4285247204
σ	0.3	– 0.0000338260
ξ	0.5	+ 0.0000214336
γ_1	$1/15$	– 0.6756036473
φ	0.5	+ 0.0000140796
γ_2	$1/2\left(1/3+1/7\right)$	– 0.0000446177

Table 2: *Sensitivity Indices of R_0*

Following the approach of [33, 34], the normalized forward sensitivity index of R_0 that depends differentially on a parameter p is defined as

$$\chi_p^{R_0} = \frac{\partial R_0}{\partial p}.\frac{p}{R_0}. \qquad (24)$$

Given this explicit formula for R_0, we can easily derive an analytical expression for the sensitivity of R_0 with respect to each parameter that comprises it. For example, the sensitivity index of R_0 with respect to the rate of social distancing, η, is

obtained as $\chi_\eta^{R_0} = \frac{\partial R_0}{\partial \eta}.\frac{\eta}{R_0} = 1.0000000010.$ (25)

Similarly, the obtained values for the sensitivity index of R_0 with respect to other parameters, for the base line parameter values in table 3 are given in Table 2 above.

From the index table, it was revealed that the most sensitive parameters are the rates of social distancing (η) and effective contact (β). Other parameters like rates of contact tracing, quarantine, isolation of cases and recovery are also sensitive to the reproduction number. By a way of illustration, $\chi_\beta^{R_0} = +1.00$ means that increasing (or decreasing) β by 10% increases (or decreases) R_0 by 10%; while $\chi_{\gamma_1}^{R_0} = -0.6756$ means that increasing (or decreasing) γ_1 by 10% decreases (or increases) R_0 by 6.756%. The interpretation of the sensitivity indices of other parameters follows as of that of β and γ_1.

Arising from this sensitivity analysis, the effects of the sensitive parameters on the dynamics of the COVID-19 model are illustrated graphically in the next section.

B. Numerical Simulations and Results

The numerical simulation for the COVID-19 model was carried out by Maple 18.0 software using direct substitution method to show solution of the model equation, the global stability of the equilibria and the effects of parameters like rates of social distancing (η), effective contact (β), contact tracing (τ_1 and τ_1), quarantine and recovery. We used some of the parameter values compatible with Corona virus as given in the Table 3 below, and by considering the initial conditions:

$s(0) = 0.3, e(0) = 0.25, q(0) = 0.2, i(0) = 0.15, j(0) = 0.1, r(0) = 0$, so that $N = 1$.

Parameters	Values	Sources
Π	273.23	[20]
μ	$3.01\text{x}10^{-5}$ day^{-1}	[20]
β	$0.62\text{x}10^{-8}$ day^{-1}	[20]
ε_1	$1.00\text{x}10^{-4}$	[35]
ε_2	$1.01\text{x}10^{-4}$	[35]
η	0.25	Assumed
τ_1	0.06	[36]
τ_2	0.07	[36]
δ_1,	0.010	[20]
δ_2	0.001	Assumed
ρ	$1/7$	[20]
θ	0.3	[35]
σ	0.3	[35]
ξ	0.5	Assumed
γ_1	$1/15$	[20]
φ	0.5	Assumed
γ_2	$1/2\left(1/3+1/7\right)$	[24]
κ	0.03	Assumed

***Table* 3:** *Parameter Values Used in the Model*

The results of the numerical simulations are given in Figures 4.1 – 4.8 to illustrate the system's behaviour for different values of the COVID-19 model's parameters.

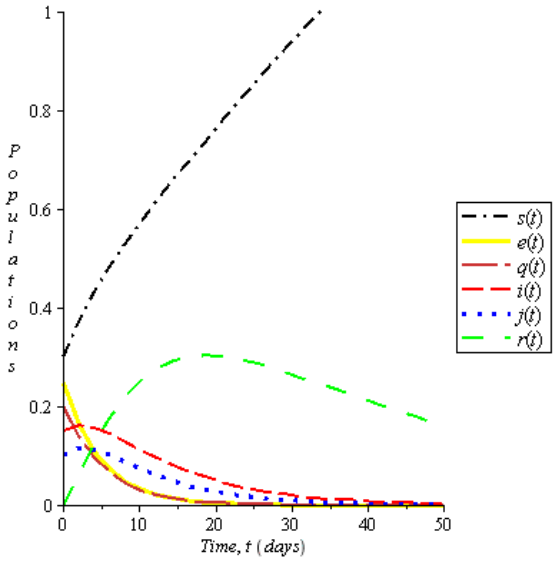

***Fig.* 2:** *Plot of all populations with time at the given model parameters*

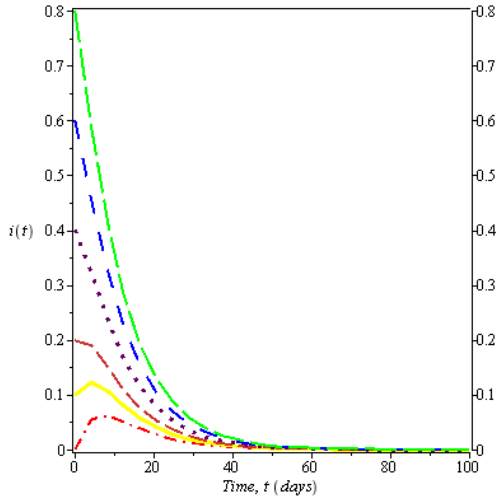

***Fig.* 3:** *Plot of the global stability if the disease-free equilibrium with various initial conditions*

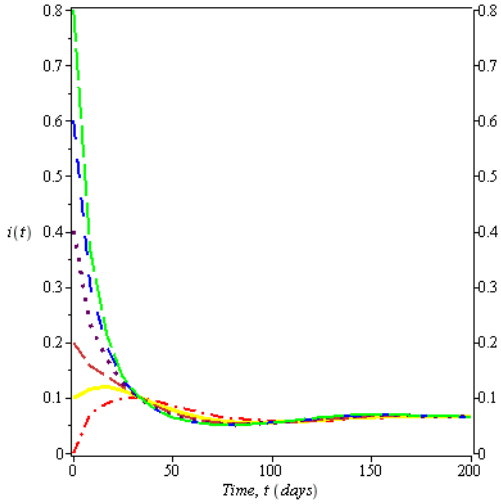

***Fig.* 4:** *Plot of the global stability if the endemic equilibrium with various initial conditions*

C. Discussion of Results

The plot in Fig.2 is the solution plot for the model equation (5). This plot shows the behaviour of the populations over time for the set of parameter values given in Table 3. It can be seen from the plot that the control measures incorporated are actually effective in reducing/eliminating COVID-19 epidemic in the population. Fig.3 and Fig.4 illustrate the global stability of the disease-free and the endemic equilibria, as established by Theorems 4 and 6 respectively. These imply that if $R_0 < 1$, elimination of COVID-19 is guaranteed regardless of the initial size of the infective and infectious individuals in the population. This is shown in Fig.3 where all solutions converge to the disease-free equilibrium. Also from Fig.4, all solutions converge to and stabilize at the endemic equilibrium, showing that irrespective of the initial size of the infective and infectious individuals in the population, COVID-19 will persist in the population whenever $R_0 > 1$. The parameter values used, shows that $\Re_0 = 3.42$ (obtained from equation (15)), which is in range when compared with [14, 15, 18-20]. However when the intervention strategies used in this model are in place, this values can be as low as $R_0 = 0.22$ (obtained from the control reproduction number in (14)).

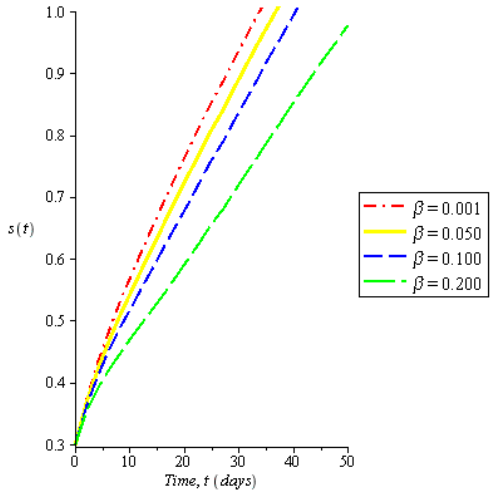

***Fig.* 5:** *Plot of the effect of contact rate, β, on the susceptible population*

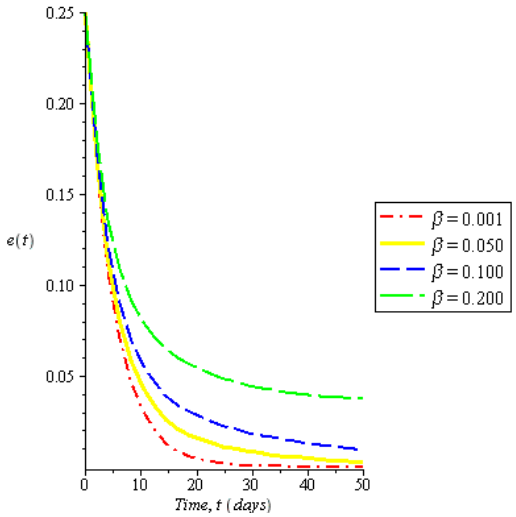

***Fig.* 6:** *Plot of the effect of contact rate, β, on the exposed population*

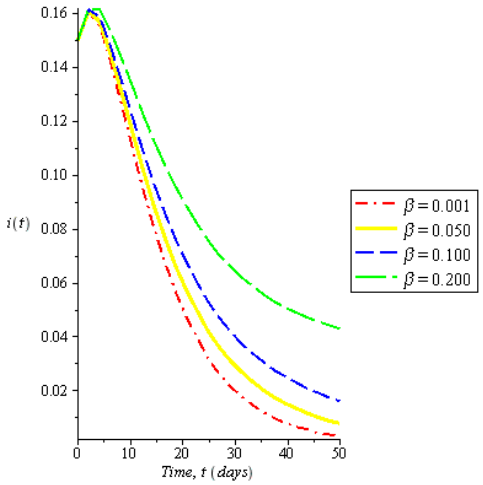

Fig. 7: *Plot of the effect of contact rate, β, on the infected population*

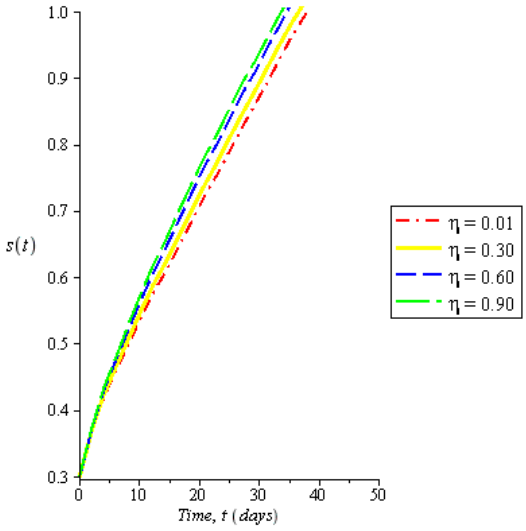

Fig. 8: *Plot of the effect of social distancing rate, η, on the susceptible population*

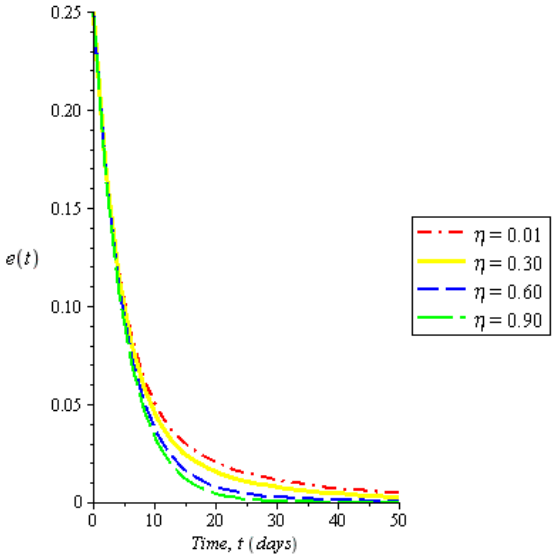

Fig. 9: *Plot of the effect of social distancing rate, η, on the exposed population*

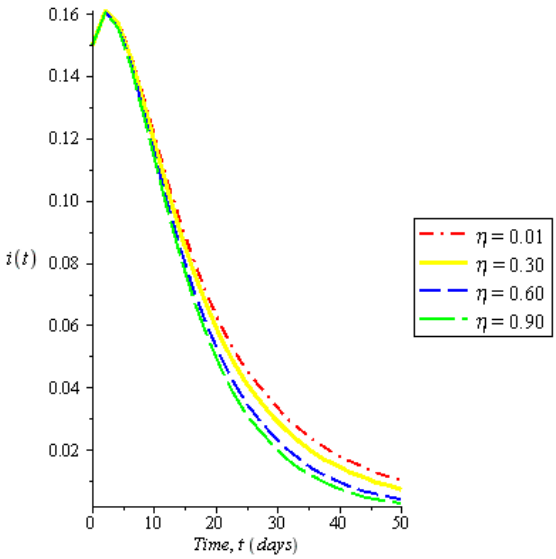

Fig. 10: *Plot of the effect of social distancing rate, η, on the infected population*

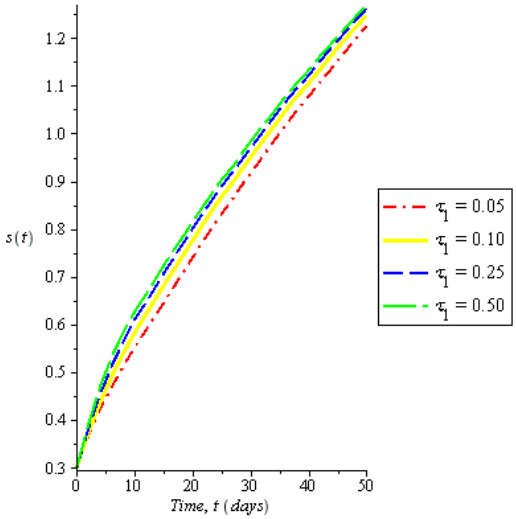

Fig. 11: *Plot of the effect of exposed contact tracing rate, τ_1, on the susceptible population*

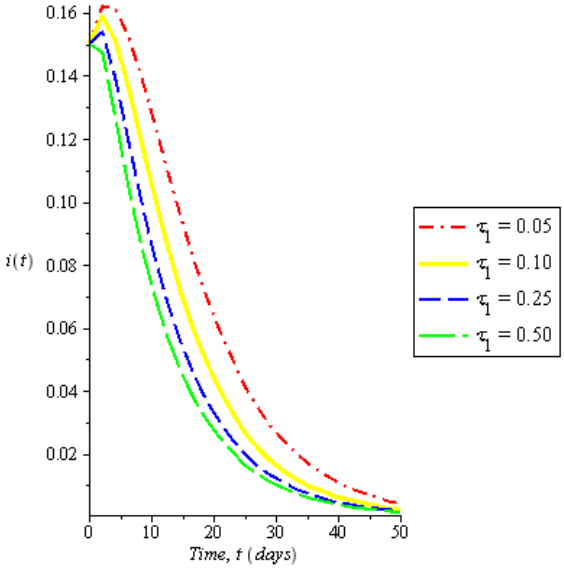

Fig. 13: *Plot of the effect of exposed contact tracing rate, τ_1, on the infected population*

Fig.5 – Fig.6 show the effect of the rate of effective contact (β) on the populations. It can be seen from Fig.5 that increase in the rate of effective contact with infectious individuals decreases the susceptible population, while increasing the exposed and infected populations as shown in Fig.6 and Fig.7 respectively. From Fig.8 – Fig.10, the rate of social distancing is shown to increase the susceptible population (in Fig.8), while reducing the exposed and infected populations in Fig.9 and Fig.10 respectively.

The plots in Fig.11 – Fig.16 illustrate the effect of contact tracing (τ_1 and τ_2) on the dynamics of COVID-19. Fig.11 and Fig.12 respectively show that increase in the rate of contact tracing increases the susceptible population, and with more increase obtained when contacts with the exposed population are traced (at a rate τ_1). Fig.13 and Fig.14 respectively show decline in the infected population when the rate of contact tracing increases, but in this case, tracing the contacts with the infected (τ_2) reduces the infected population faster.

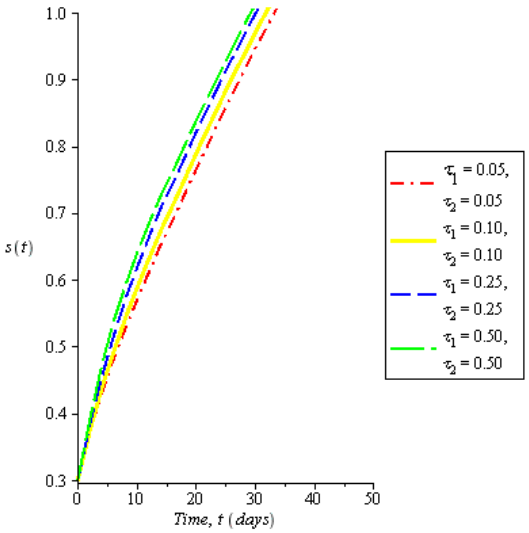

***Fig.* 15:** *Plot of the effect of combined contact tracing rate, τ_1 and τ_2, on the susceptible population*

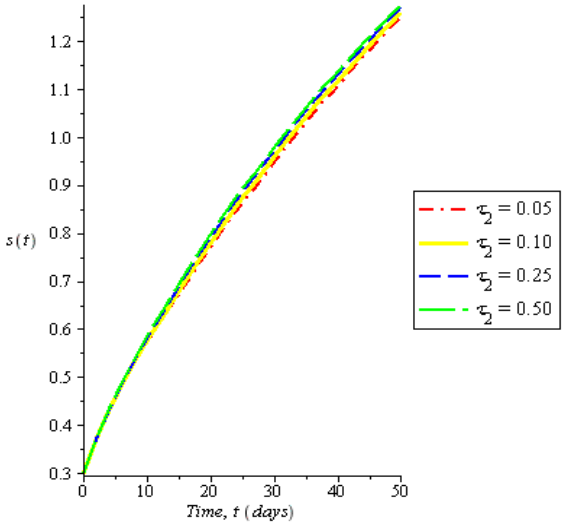

***Fig.* 12:** *Plot of the effect of infected contact tracing rate, τ_2, on the susceptible population*

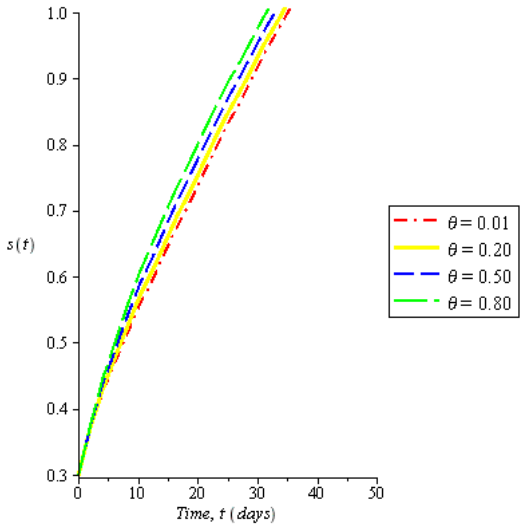

***Fig.* 17:** *Plot of the effect of quarantine rate, θ, on the susceptible population*

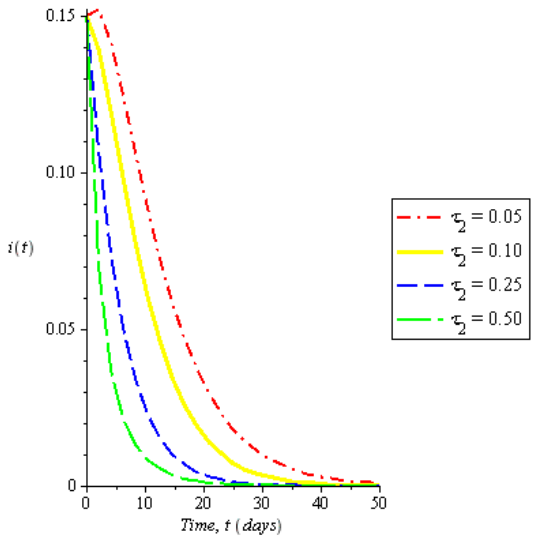

***Fig.* 14:** *Plot of the effect of infected contact tracing rate, τ_2, on the infected population*

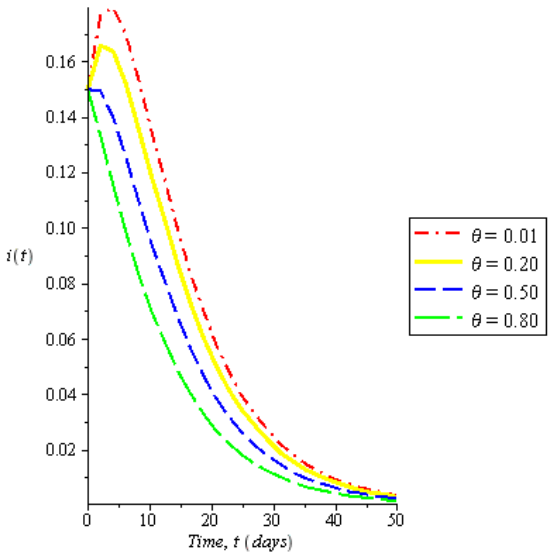

***Fig.* 19:** *Plot of the effect of quarantine rate, θ, on the infected population*

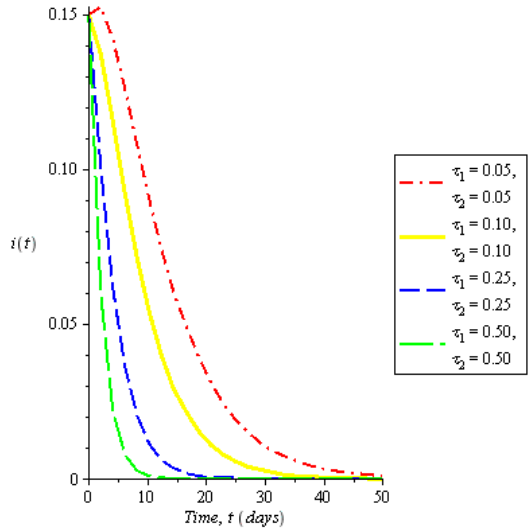

***Fig.* 16:** *Plot of the effect of combined contact tracing rate, τ_1 and τ_2, on the infected population*

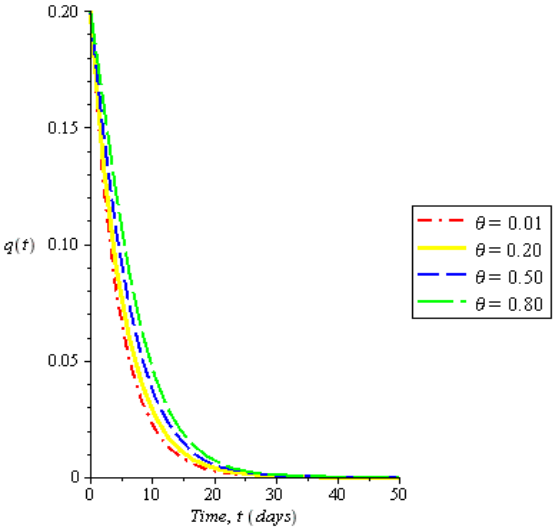

***Fig.* 18:** *Plot of the effect of quarantine rate, θ, on the quarantined population*

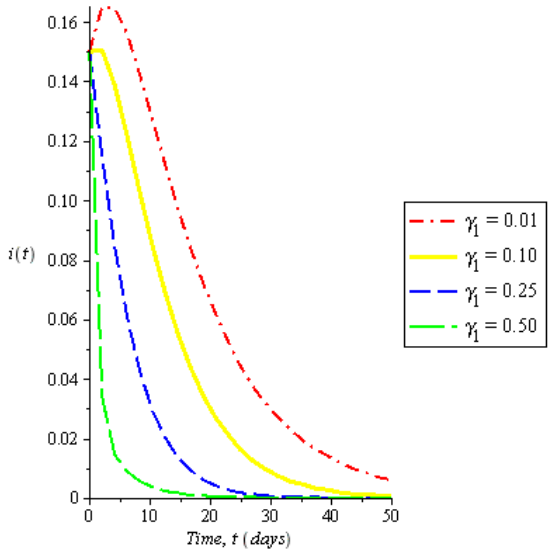

***Fig.* 20:** *Plot of the effect of recovery rate, γ_1, on the infected population*

The combined effect of both τ_1 and τ_2 are investigated, and the results as depicted by Fig.15 and Fig.16 respectively show that the susceptible population increases more, while the infected population declines faster when the two forms of contact tracing are considered together.

The effect of the rate of quarantine (θ) was also verified and the results are shown in Fig.17 – Fig.19. From Fig.17 and Fig.18, it was shown that increase in the rate of quarantine increases the susceptible population as well as the quarantine population respectively, while reducing the infected population as shown in Fig.19.

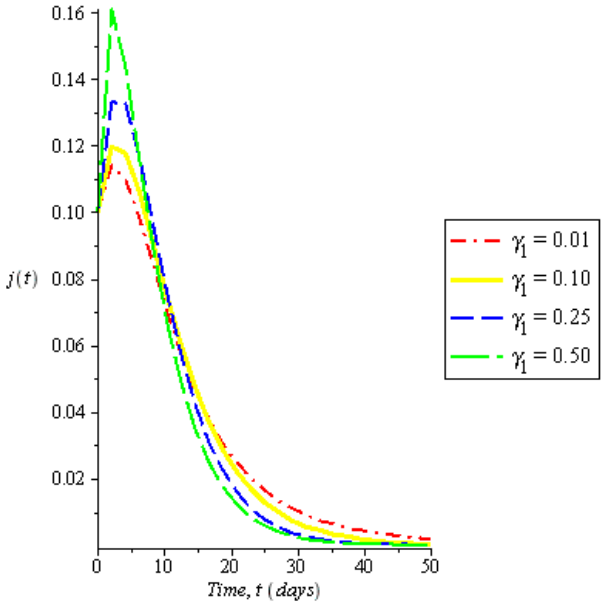

***Fig.* 21:** *Plot of the effect of recovery rate, γ_1, on the isolated population*

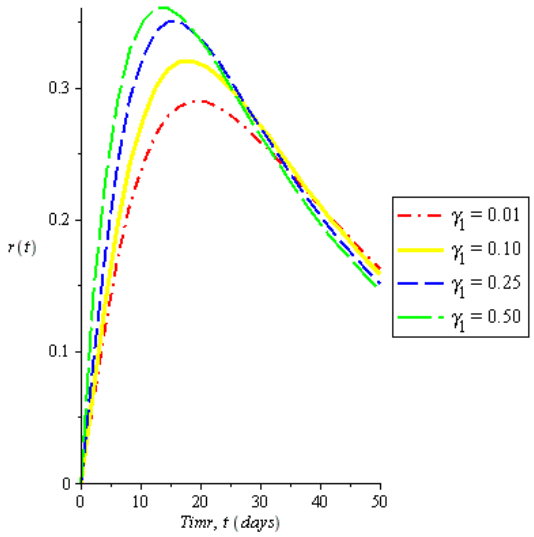

***Fig.* 23:** *Plot of the effect of recovery rate, γ_1, on the recovered population*

Furthermore, it was shown in Fig.20 that there is a sharp decrease in the infected population when the rate of recovery (γ_1) increases. Also, this increase initially increases the isolated population, which later declines since some individuals progress out of this population upon recovery. This is depicted by Fig.21. From Fig.22, the effect of supportive treatment (γ_2) was seen, which is administered to the individuals in isolation centres. As this rate of treatment increases, there is a decrease in the isolated population as such individuals progress unto the recovered population. From Fig.23 and Fig.24, it was shown that both recovery rate and supportive treatment rate respectively increases the recovered population initially. However at a point in time, the recovered population declines in both cases. This can be attributed to the fact that recovered individuals lose their immunity (at a rate κ) and move to the susceptible population where they can be re-infected.

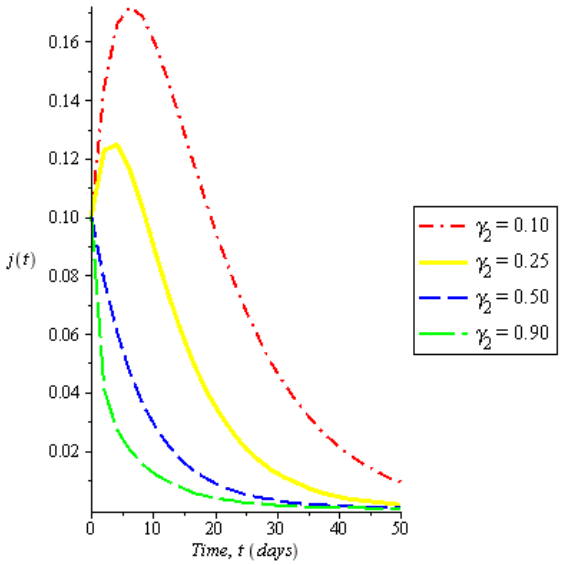

***Fig.* 22:** *Plot of the effect of supportive treatment rate, γ_2, on the infected population*

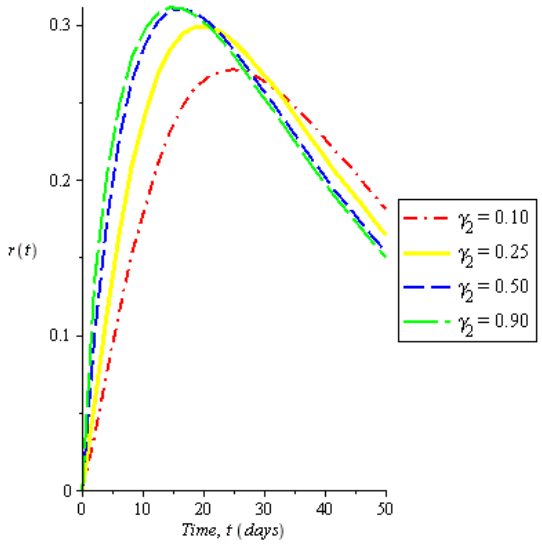

***Fig.* 24:** *Plot of the effect of supportive treatment rate, γ_2, on the recovered population*

V. CONCLUSION

In this paper, we formulated and analysed an epidemic model for COVID-19, in which intervention strategies like social distancing, contact tracing, quarantine, isolation of cases and supportive treatment are considered. The region where the model is epidemiologically feasible and mathematically well-posed was established, and the existence and stability of both disease-free and endemic equilibria were determined to depend on the threshold value, R_0.

Sensitivity analysis was performed on R_0 and showed that rate of social distancing (η) and rate of effective contact (β) are the most sensitive parameters to the reproduction number (R_0). Therefore, intervention strategies should be targeted towards these two parameters, among others, so that the spread of the disease would be reduced. The rate of contact could be reduced by increasing the rate of social distancing in the population. To achieve this, measures such as lockdown to restrict movement of people, introduction of travel control measures, ban on public gatherings, closure of schools and workplaces (coupled with learn and work from home plans), and so on, can be put in place.

From the result of the numerical simulations, it is recommended that any individuals who have any form of recent contact with confirmed cases/exposed individuals be traced accordingly and quarantined/isolated immediately as the case may be. Furthermore, medical/health practitioners should take all necessary precautions (so as to prevent them from contracting COVID-19) while administering supportive treatment/care to infective individuals in isolation centres to enhance their quick recovery.

Most importantly, corona virus's vaccines as well as antiviral drugs should be designed in order to combat the current as well as possible future COVID-19 epidemics.

ACKNOWLEDGMENT

The authors express thanks to the anonymous referees whose comment led to this improved paper.

REFERENCES

[1] World Health Organization. WHO Statement Regarding Cluster of Pneumonia Cases in Wuhan, China, 2020. https://www.who.int/china/news/detail/09-01-2020-\who-statement-regarding-cluster-of-pneumonia-cases-in-wuhan-china.

[2] Q. Li, X. Guan, P. Wu, X.Z. Wang, L. Wou, Y. Tong, *et al*. Early Transmission dynamic in Wuhan, china of novel corona virus infected pneumonia. N. Engl. Med. 2020. https://doi.org/10.1056/NEJM092001316.

[3] World Health Organization. Origin of Severe Acute Respiratory Syndrome Coronavirus 2 (SARS-CoV-2). 2020.
Retrieved 02/20/2020.
[4] C. Roth, M. Schunk, P. Sothmann, *et al*. Transition of 2019-CoV infection from an asymptotic contact in Germany. N. Engl. J. Med. 2020. https://doi.org/1056/2001468.
[5] S.A. Lauer, K.H. Grantz, Bi . The incubation period of corona virus disease 2019 (COVID 19) from publicly reported confirmed cases: Estimation and Application. 2020.
[6] M. Meselson. Droplets and Aerosol in the Transmission of Severe Acute Respiratory Syndrome Corona virus 2 (SARS-CoV-2). N Engl. J. Med. 2020. Doi: 10/1056/NEJM Mc 2009384.
[7] H. Zhang, Z.J. Kang, H.Y. Gong, *et al*. The digestive system is a potential route of 2019-CoV infection. Jama. bioRxiv. 2020. Doi:10:1101/2020.10.30.927806.
[8] L.T. Phang, T.V. Nguyen, *et al*. Importation and human to human transmission of the novel corona virus in Vietnam, N. Engl. J Med. 2020. Doi: 10:1056/NEJM 2001272.
[9] Health line Media. Everything you need to know about the 2019 corona virus and COVID-19. Healthline.com. published March 25, 2020.
[10] World Health Organization updates COVID-19 dashboard with better data visualization. 2020 WHO Retrieved 23 April 2020.
[11] O. Cao, Q. Zhang, X. Lu, D. Pfeiffer, Z. Jia, Song. Estimating the effective reproduction number of the 2019-nCoV in China. MedRxiv. 2020.
[12] World Health Organization. Media Briefing to update the public on the COVID-19 outbreak 17 April, 2020. Weforum.org
[13] P.G.T. Walker, C. Whittaker, O. Watson, M. Baguelin, N.M. Ferguson, *et al*. Report 12- The global impact of COVID-19 an strategies for mitigation and suppression. Imperial College London. MRC Centre for Global Infectious Disease Analysis. 2020
[14] A.J. Kucharski, T.W. Russell, C. Diamond, Y. Liu, J. Edmunds, S. Funk, R.M. Eggo. Early dynamics of transmission and control of COVID-19: a mathematical modelling study. Lancet Infect Dis. 2020. dio: https://doi.org/10.1016/S1473-3099(20)30144-4.
[15] B. Tang, X. Wang, Q. Li, N.L. Bragazzi, S. Tang, Y . Xiao, and W. Jianhong. Estimation of the transmission risk of 2019-nCoV and its implication for public health intervention. J. Clin. Med. 2020. 9(2020) p.462.
[16] B. Tang, N.L. Bragazzi, Q. Li, S. Tang, Y. Xiao, and W. Jianhong. Estimation of the transmission risk of novel corona virus (2019-nCoV). J. Clin. Med. 5(2020) pp.248-255. 2020.
[17] V.A. Okhuese. Mathematical predictions for COVID-19 as a global pandemic. MedRxiv. 2020. https://doi.org/10.1101/2020.03.19.20038794.
[18] J.T. Wu, K. Leung, G.M. Leung. Nowcasting and forecasting the potential domestic and international spread of the 2019-nCoV outbreak originating in Wuhan, China: a modelling study, *Lancet*, **395**: 689–697. 2020.
[19] J. M. Read, J. R. E. Bridgen, D. A. T. Cummings, A. Ho, C. P. Jewell. Novel coronavirus 2019-nCoV: early estimation of epidemiological parameters and epidemic predictions, *medRxiv*. 2020.
[20] C. Yang, and J. Wang. A mathematical model for the novel coronavirus epidemic in Wuhan, China, *Mathematical Biosciences and Engineering*, **17**(3): 2708-2724. 2020. Doi: 10.3934/mbe.2020148.
[21] N. Imai, A. Cori, I. Dorigatti, M. Baguelin, C. A. Donnelly, S. Riley, *et al.* Report 3: Transmissibility of 2019-nCoV, 2020. Available from: https://www.imperial.ac.uk/mrc-global-infectious-disease-analysis/news--wuhan-coronavirus/.
[22] H. Zhu, Q. Gao, M. Li, C. Wang, Z. Feng, P. Wang, *et al.* Host and infectivity prediction of Wuhan 2019 novel coronavirus using deep learning algorithm, *bioRxiv*. 2020.
[23] J.F.W. Chan, S. Yuan, K.H. Kok, K.K.W. To, H. Chu, J. Yang, *et al.* A familial cluster of pneumonia associated with the 2019 novel coronavirus indicating person-to-person transmission: a study of a family cluster, *Lancet*, **395**: 514–523. 2020.
[24] K. Prem, Y. Liu, T.W. Russell, A.J. Kucharski, R.M. Eggo, N. Davies, Centre for the Mathematical Modelling of Infectious Diseases COVID-19 Working Group, M. Jit, P. Klepac. The effect of control strategies that reduce social mixing on outcomes of the COVID-19 epidemic in Wuhan, China, medRxiv 2020. preprint doi: https://doi.org/10.1101/2020.03.09.20033050.
[25] World Health Organization: Coronavirus Disease 2019 (COVID-19) Situation Report – 73, WHO April, 2 2020. https://www.who.int/docs/default-source/coronavirus/situation-reports/20200402-sitrep-73-covid-19.pdf.
[26] R. M. Burke, C. M. Midgley, A. Dratch, M. Fenstersheib, T. Haupt, M. Holshue, *et al.* Active monitoring of persons exposed to patients with confirmed COVID-19 — United States, January–February 2020. *MMWR Morb Mortal Wkly Rep*. doi : 10.15585/mmwr.mm6909e1external icon.
[27] P. Van-den-Driessche, J. Watmough, Reproduction Number and Sub-threshold Endemic Equilibria for Computational Models of Diseases Transmission; *Mathematical Bioscience*, 180 (2002): 29-48.
[28] O. Diekmann, J.A.P. Heesterbeek, J.A.J. Metz. On the Definition and the Computation of the Basic Reproduction Ratio, R_0 in Models for Infectious diseases in Heterogeneous Population, *J. Math. Biol*. 28 (1990): 365-382.
[30] C. Castillo-Chavez, Z. Feng, and W. Huang. On the Computation of R_0 and its Role on Global Stability. 2001.
[29] O. Diekmann, J.A.P. Heesterbeek. Mathematical Epidemiology of Infectious Diseases: Model Building, Analysis and Interpretation. Wiley, New York. 2000.
[31] J.P. LaSalle. The Stability of Dynamical systems, Regional conference Series in Applied Mathematics, SIAM, Philadelphia 1976.

[32] C.V. De-Leon. Construction of Lyapunov Functions for Classics SIS, SIR and SIRS Epidemic Model with Variable Population Size. *Unite Academia de Mathematicas, Universidadn Autonoma de Guerrere, Mexico Facultad de Estudios Superiores Zarogoza*, UNAM, Mexico. 2009

[33] T.O. Oluyo and M.O. Adeyemi. Sensitivity Analysis of Zika Epidemic Model. *International Journal of Scientific and Engineering Research,* **9**(2). 2018 : 587-601.

[34] J.O. Akanni, F.O Akinpelu, S. Olaniyi, A.T. Oladipo and A.W. Ogunsola. Modelling Financial Crime Population Dynamics: Optimal Control and Cost-effectiveness Analysis, *International Journal of Dynamics and Control*, 2019. https://doi.org/10.007/s40435-019-00572-3.

[35] T. Berge, A. J. Ouemba Tassé, H. M. Tenkam, J. Lubuma. Mathematical modeling of contact tracing as a control strategy of Ebola Virus Disease, *Ebola.IJB.R1.* (2018). pp.1-35.

[36] C.E. Madubueze, A.R. Kimbir and T. Aboiyar. Global stability of Ebola Virus Disease Model with contact tracing and Quarantine, *Applications and Applied Mathematics*, **13**(1). 2018: 382-403.